

# Proposal for reversing the weak measurement with arbitrary maximum photon number

Xiaodong Zeng,<sup>1,2,3</sup> M. Al-Amri,<sup>1,2,3</sup> Shiyao Zhu,<sup>3</sup> and M. Suhail Zubairy<sup>1</sup>

<sup>1</sup>*Institute for Quantum Science and Engineering (IQSE) and Department of Physics and Astronomy, Texas A&M University, College Station, Texas 77843-4242, USA*

<sup>2</sup>*The National Center for Applied Physics, KACST, P.O. Box 6068, Riyadh 11442, Saudi Arabia*

<sup>3</sup>*Beijing Computational Science Research Center, Beijing 100084, China*

(Received 15 June 2015; published 20 May 2016)

We present a proposal for reversing the weak (partial-collapse) quantum measurement on a cavity field with arbitrary maximum photon number. We start by putting forth a protocol to realize quantum PHASE gates between the cavity field and an ancilla qubit. Afterward, adopting these PHASE gates and some other quantum gates, we can determine the reversal of the cavity state just by observing the ancilla qubit. Compared to previous proposals, our proposal does not need any other weak measurement and can save reversal time, which is significantly important in quantum informatics and quantum computation.

DOI: [10.1103/PhysRevA.93.053826](https://doi.org/10.1103/PhysRevA.93.053826)

## I. INTRODUCTION

Weak measurement has attracted a great deal of attention in the past decade in both theory and experiment [1–25]. Compared to traditional quantum projection measurement [26], weak measurement is related to the condition that correlation between the quantum state and the measuring device (meter) is very weak. Consequently, the initial state does not fully collapse after such a measurement and quantum information of the initial state is partially conserved. We have therefore a finite probability to collect the initial-state information retained in the final state. Weak measurement and quantum measurement reversal can play an important role in many quantum phenomena [4–17]. For example, in Refs. [5–7], it was shown that weak measurement and the reversal can effectively suppress amplitude-damping decoherence for a single qubit; Refs. [10–12] showed that quantum entanglement can be greatly protected by weak measurement and the reversal. As a result, how to reverse weak measurement physically becomes useful and important.

There have been several proposals to reverse weak measurement [18–25]. Most of them provide reversal of qubit states and require another weak measurement in the reversal process. In our previous work [22] we were able to reverse a general state of the type  $\sum_{n=0}^{n_{\max}} \alpha_n |n\rangle$ . Additionally, our scheme in Ref. [25] based on quantum logical gates can avoid another weak measurement and make the protocol faster.

In an earlier work [22], we assumed that the original cavity state is in a state  $\sum_{n,m=0}^{n_{\max}} \rho_{nm} |n\rangle\langle m|$ . After the weak measurement, it evolves into  $\sum_{n,m=0}^{n_{\max}} \rho_{nm} e^{-(n+m)\gamma t} |n\rangle\langle m|$ . Our reversal proposal mainly contains the following steps. The first step is to swap the components symmetrically from  $\sum_{n,m=0}^{n_{\max}} \rho_{nm} e^{-(n+m)\gamma t} |n\rangle\langle m|$  to  $\sum_{n,m=0}^{n_{\max}} \rho_{nm} e^{-(n+m)\gamma t} |N-n\rangle\langle N-m|$ , where  $N$  is an adjustable parameter that is bigger than or equal to the maximum photon number  $n_{\max}$  and  $\gamma$  is the cavity decay rate. The second step is to do a weak measurement on the cavity. This transforms the state to be  $\sum_{n,m=0}^{n_{\max}} \rho_{nm} e^{-2N\gamma t} |N-n\rangle\langle N-m|$ , which has a common coefficient  $e^{-2N\gamma t}$  and can be dropped after normalization. Third, we repeat the first step on the state in order to transfer the symmetrical state to the initial state  $\sum_{n,m=0}^{n_{\max}} \rho_{nm} |n\rangle\langle m|$ . Because the second null-result weak measurement has a

probability to fail, we reverse the quantum state successfully with only some probability. The drawback of this method is that the second weak measurement sometimes takes a long time [22], which makes the reversal process slow.

In another work [25], an ancilla qubit is used to interact with the cavity field to construct a controlled-NOT (CNOT) gate and then the atom is detected. If the ancilla qubit is found in the ground state, the cavity state is projected to the original state and the weak measurement is reversed. This proposal does not need a second weak measurement. Therefore, it takes less time. However, this scheme can only solve the problem when the cavity has at most one photon.

In the present paper we combine these ideas to present a protocol to reverse the cavity state with arbitrary maximum photon number without carrying out another weak measurement. Our protocol requires a series of CNOT gates to accomplish the reversal for this generalized state by extending the method presented in [25]. The key is to construct quantum PHASE gates between the cavity field and an ancilla qubit. We just need to do a generalized measurement on the ancilla qubit to project the cavity state to the original state. No weak measurement needed here means that our proposal can save the reversal time even for a high-dimensional system. This is very important in many applications, such as quantum computation and quantum entanglement protection.

The paper is organized as follows. In Sec. II we present the mathematical formalism of our protocol. In Sec. III we construct quantum PHASE gates. In Sec. IV we use PHASE gates and Hadamard gates to construct CNOT gates and then reverse the quantum state after a weak measurement. Finally, we summarize our work in Sec. V.

## II. REVERSING THE WEAK MEASUREMENT

We consider the schematic diagram shown in Fig. 1 for the implementation of our protocol to reverse the weak measurement. The cavity field is initially in a pure state written as

$$|\varphi_0\rangle = \sum_{n=0}^{n_{\max}} \alpha_n |n\rangle, \quad (1)$$

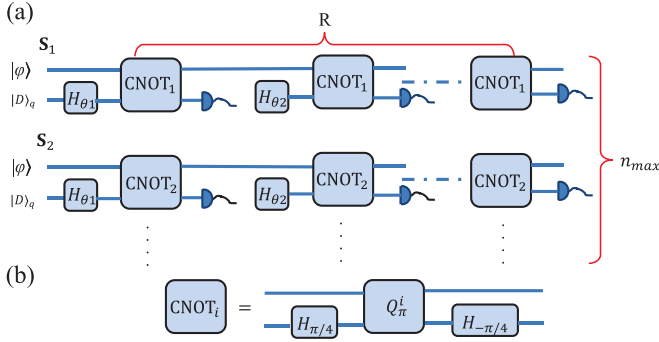


FIG. 1. (a) Schematic diagram of the proposal. Initially, the cavity state  $|\varphi\rangle$  shown in Eq. (2) is input to process  $S_1$  and the process  $S_1$  can reverse the cavity state to the state shown in Eq. (6) with some probability. Then the cavity state  $|\varphi\rangle$  shown in Eq. (6) is input to process  $S_2$  and the process  $S_2$  can reverse the cavity state to the state shown in Eq. (11) with some probability. After processes  $S_1 \rightarrow S_{n_{\max}}$ , the cavity state can be reversed to the original state shown in Eq. (1). Here  $H_{\theta_j}$  ( $j = 1, 2, \dots, R$ ) can prepare the ancilla qubit from  $|D\rangle_q$  to  $\cos\theta|D\rangle_q + \sin\theta|U\rangle_q$  with  $\tan\theta = e^{2j-1}\gamma t$ . The  $\text{CNOT}_i$  ( $i = 1, 2, \dots, n_{\max}$ ) are CNOT gates of Eq. (4) with the bases  $(\sum_{n=0}^{i-1} \alpha_n e^{-n\gamma t} |n\rangle)|D\rangle_q$ ,  $(\sum_{n=0}^{i-1} \alpha_n e^{-n\gamma t} |n\rangle)|U\rangle_q$ ,  $(\sum_{n=i}^{n_{\max}} \alpha_n e^{-n\gamma t} |n\rangle)|D\rangle_q$ , and  $(\sum_{n=i}^{n_{\max}} \alpha_n e^{-n\gamma t} |n\rangle)|U\rangle_q$ . (b) The CNOT gates consist of two Hadamard gates and one PHASE gate. The PHASE gate  $Q_\pi^i$  denotes that only when the photon number in the cavity is bigger than or equal to  $i$  and the ancilla qubit is in the excited state  $|U\rangle_q$  can there be a  $\pi$  phase shift.

which satisfies the normalization condition  $\sum_{n=0}^{n_{\max}} |\alpha_n|^2 = 1$ . We assume that there is an ideal photon detector outside the cavity, which can capture all the photons escaping from the cavity. If there is no click, the final state evolves into [22,27,28]

$$|\varphi\rangle = \left( \sum_{n=0}^{n_{\max}} \alpha_n e^{-n\gamma t} |n\rangle \right) / \Lambda_0 \quad (2)$$

according to the quantum trajectory theory. Here  $\Lambda_0 = (\sum_{n=0}^{n_{\max}} |\alpha_n|^2 e^{-2n\gamma t})^{1/2}$  is the normalization factor and  $\gamma$  is the cavity decay rate. For simplicity, we ignore  $\Lambda_0$  here. The schematic diagram is shown in Fig. 1(a). Following the method in Ref. [25], we add an ancilla qubit prepared in the state  $\cos\theta|D\rangle_q + \sin\theta|U\rangle_q$  to interact with the cavity field. Here  $|D\rangle_q$  and  $|U\rangle_q$  are two eigenstates of the ancilla qubit. Initially, the cavity field and the ancilla qubit are in the following state:

$$\left( \sum_{n=0}^{n_{\max}} \alpha_n e^{-n\gamma t} |n\rangle \right) \otimes (\cos\theta|D\rangle_q + \sin\theta|U\rangle_q). \quad (3)$$

Here we assume that  $\sum_{n=1}^{n_{\max}} \alpha_n e^{-n\gamma t} |n\rangle$  is a hypothetical eigenstate and consider  $\sum_{n=0}^{n_{\max}} \alpha_n e^{-n\gamma t} |n\rangle$  to be a superposition state of  $\alpha_0|0\rangle$  and  $\sum_{n=1}^{n_{\max}} \alpha_n e^{-n\gamma t} |n\rangle$ . The next step is to operate the CNOT gate

$$\begin{pmatrix} 1 & 0 & 0 & 0 \\ 0 & 1 & 0 & 0 \\ 0 & 0 & 0 & 1 \\ 0 & 0 & 1 & 0 \end{pmatrix} \quad (4)$$

on the state of Eq. (3). The basis of the matrix are  $|0\rangle|D\rangle_q$ ,  $|0\rangle|U\rangle_q$ ,  $(\sum_{n=1}^{n_{\max}} \alpha_n e^{-n\gamma t} |n\rangle)|D\rangle_q$ , and

$(\sum_{n=1}^{n_{\max}} \alpha_n e^{-n\gamma t} |n\rangle)|U\rangle_q$ . After the operation, the state evolves into

$$\begin{aligned} & \left[ \alpha_0 \cos\theta|0\rangle + \left( \sum_{n=1}^{n_{\max}} \alpha_n e^{-(n-1)\gamma t} |n\rangle \right) e^{-\gamma t} \sin\theta \right] \otimes |D\rangle_q \\ & + \left[ \alpha_0 \sin\theta|0\rangle + \left( \sum_{n=1}^{n_{\max}} \alpha_n e^{-(n-1)\gamma t} |n\rangle \right) e^{-\gamma t} \cos\theta \right] \\ & \otimes |U\rangle_q. \end{aligned} \quad (5)$$

We set  $\tan\theta = e^{\gamma t}$  and make a projecting measurement on the ancilla qubit. The cavity will be projected to

$$|\varphi\rangle = \alpha_0|0\rangle + \left( \sum_{n=1}^{n_{\max}} \alpha_n e^{-(n-1)\gamma t} |n\rangle \right) \quad (6)$$

when the outcome is  $|D\rangle_q$  and

$$|\varphi\rangle = \alpha_0|0\rangle + \left( \sum_{n=1}^{n_{\max}} \alpha_n e^{-(n-1)\gamma t} |n\rangle \right) e^{-2\gamma t} \quad (7)$$

when the outcome is  $|U\rangle_q$ . If we get  $|U\rangle_q$ , we repeat the above procedures but set  $\tan\theta = e^{2\gamma t}$  initially. Similarly, the measurement result  $|D\rangle_q$  or  $|U\rangle_q$  will project the cavity to

$$|\varphi\rangle = \alpha_0|0\rangle + \left( \sum_{n=1}^{n_{\max}} \alpha_n e^{-(n-1)\gamma t} |n\rangle \right) \quad (8)$$

or

$$|\varphi\rangle = \alpha_0|0\rangle + \left( \sum_{n=1}^{n_{\max}} \alpha_n e^{-(n-1)\gamma t} |n\rangle \right) e^{-4\gamma t}, \quad (9)$$

respectively. We can repeat these procedures  $R$  times in order for the cavity to evolve into the state of Eqs. (6) and (8) with a finite probability less than 1 [25].

So far, we removed a common coefficient  $e^{-\gamma t}$  of the hypothetical excited state  $\sum_{n=1}^{n_{\max}} \alpha_n e^{-n\gamma t} |n\rangle$ . Now we assume this state of Eq. (8) to be the superposition state of  $\alpha_0|0\rangle + \alpha_1|1\rangle$  and  $\sum_{n=2}^{n_{\max}} \alpha_n e^{-(n-1)\gamma t} |n\rangle$ . In a similar manner, we also need an ancilla qubit to interact with the cavity and a quantum CNOT gate of Eq. (4) to manage the cavity and ancilla qubit. After the operation, the whole state of the cavity field and the ancilla qubit reads

$$\begin{aligned} & [(\alpha_0|0\rangle + \alpha_1|1\rangle) \cos\theta \\ & + \left( \sum_{n=2}^{n_{\max}} \alpha_n e^{-(n-2)\gamma t} |n\rangle \right) e^{-\gamma t} \sin\theta] \otimes |D\rangle_q \\ & + [(\alpha_0|0\rangle + \alpha_1|1\rangle) \sin\theta \\ & + \left( \sum_{n=2}^{n_{\max}} \alpha_n e^{-(n-2)\gamma t} |n\rangle \right) e^{-\gamma t} \cos\theta] \otimes |U\rangle_q. \end{aligned} \quad (10)$$

We repeat the procedures of Eqs. (6)–(9). After  $R$  times, we can get the following state with some probability:

$$|\varphi\rangle = \alpha_0|0\rangle + \alpha_1|1\rangle + \alpha_2|2\rangle + \left( \sum_{n=3}^{n_{\max}} \alpha_n e^{-(n-2)\gamma t} |n\rangle \right). \quad (11)$$

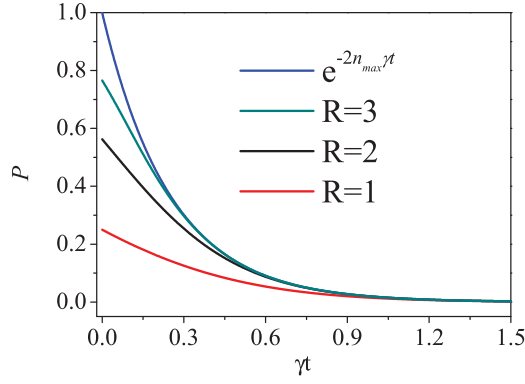


FIG. 2. Success probability for  $R = 1, 2, 3$  compared with the curve  $e^{-2n_{\max}\gamma t}$  (from bottom to top). Here we set  $n_{\max} = 2$ .

Successfully, we remove another common coefficient  $e^{-\gamma t}$  of the hypothetical excited state  $\sum_{n=2}^{n_{\max}} \alpha_n e^{-n\gamma t} |n\rangle$ . After  $n_{\max}$  times of the above process, we can reverse the state of Eq. (2) back to the initial state of Eq. (1). In the following, we calculate the total success probability for the reversal process. To remove each  $e^{-\gamma t}$ , the success probability is [25]

$$P_1 = p_1 + (1 - p_1)p_2 + (1 - p_1)(1 - p_2)p_3 + \dots + (1 - p_1) \dots (1 - p_{R-1})p_R, \quad (12)$$

where

$$p_j = (\cos \theta)^2 = \frac{e^{-2^j \gamma t}}{1 + e^{-2^j \gamma t}} \quad (13)$$

is the probability to observe the ancilla qubit in  $|D\rangle_q$  for the  $j$ th observation. As shown in Ref. [25], if  $\gamma t$  is not very small, the first few  $p_j$  dominate  $P_1$  and

$$P_1 \approx e^{-2\gamma t}. \quad (14)$$

After  $n_{\max}$  times of the above procedures, the total success probability is the product of the probability of each step

$$P \rightarrow e^{-2n_{\max}\gamma t}. \quad (15)$$

In Fig. 2 we plot the success probability of our proposal as a function of  $\gamma t$ , where  $n_{\max} = 2$ . This shows that as  $R$  increases, the probability approaches  $e^{-2n_{\max}\gamma t}$ . Compared to the previous schemes [21,22], our proposal has no advantage in the success probability. The most important advantage of our proposal is that we do not need another weak measurement and can make the protocol faster

### III. QUANTUM PHASE GATE WITH ARBITRARY MAXIMUM PHOTON NUMBER

In this section we present how to realize the quantum PHASE gates physically, which are necessary to construct the CNOT gates used in the previous section [see Fig. 1(b)]. Similar to Ref. [25], we can utilize the cavity and an ancilla qubit to construct the PHASE gate. However, in the present proposal, it is hard to control the interaction time between the cavity and the ancilla qubit to obtain a suitable phase shift. The reason is that the phase shift is related to the Rabi frequency, which in turn is dependent on the cavity photon number. We need to divide

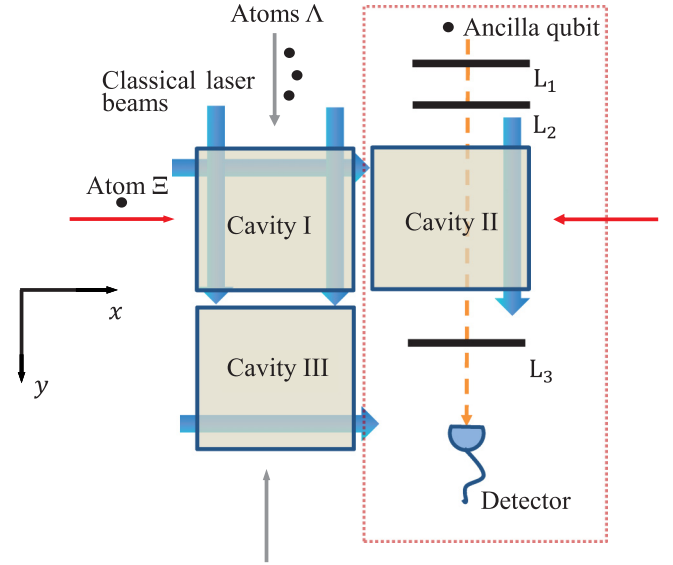


FIG. 3. Protocol diagram showing the three cavities I, II, and III in Figs. 5 and 7. The wide blue arrows are classical laser beams. Atom  $\Xi$  can pass through cavities I and II, while atoms  $\Lambda$  can pass through cavities I and III. The dotted box of the right part is the same apparatus as that in Refs. [25,31]. Here  $L_1$ ,  $L_2$ , and  $L_3$  are three Ramsey laser fields:  $L_1$  can prepare the initial state of the ancilla qubit [ $H_{\theta_j}$  in Fig. 1(a)], while  $L_2$  and  $L_3$  can do Hadamard gates on the ancilla qubit [ $H_{\pi/4}$  and  $H_{-\pi/4}$  in Fig. 1(b)]. The detector can measure the state of the ancilla qubit.

the cavity state into a hypothetical ground state  $\sum_0^s \alpha_n e^{-n\gamma t} |n\rangle$  and an excited state  $\sum_{s+1}^{n_{\max}} \alpha_n e^{-n\gamma t} |n\rangle$ , where  $s$  is an adjustable integer that is smaller than  $n_{\max}$ . Furthermore, we require that only when the cavity photon number is bigger than  $s$  and the ancilla qubit is in the excited state can there be a phase shift.

#### A. Setup and basic steps

Our protocol is sketched in Fig. 3. Cavity I contains the field state shown in Eq. (2) initially and has two resonant frequencies, i.e.,  $\omega_e$  and  $\omega_a$  [29,30], which also can be considered as two near single-mode cavities. We assume that the initial field frequency of cavity I is  $\omega_e$ . The cavity structure is shown in Fig. 5. Our objective is to use the setup shown in Fig. 3 to reverse the state of cavity I back to the initial state shown in Eq. (1) without a weak measurement. However, in Ref. [22], after the cavity state has been swapped with the symmetric state by driving atoms to pass through the cavity, we need to monitor the cavity by an ideal detector, which is called the second weak measurement if there is no click. At last we drive atoms to pass through the cavity again to swap the cavity state with the initial state shown in Eq. (1). The second weak measurement always takes a long time, which is harmful to the quantum information process.

In addition to the target cavity I, we also need two other cavities, denoted by II and III. Both II and III have the resonant frequency  $\omega_e$ . The three cavities are arrayed in the  $x$ - $y$  plane. We also need two kinds of atoms, denoted by atom  $\Xi$  and atom  $\Lambda$  as shown in Fig. 4. There are classical Gaussian beams propagating through the cavities with directions perpendicular

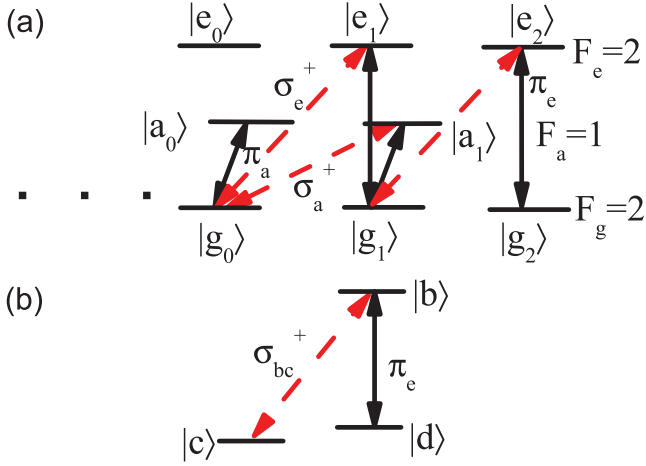


FIG. 4. (a) Structure of atom  $\Xi$ . The total angular momenta of degenerate levels  $|e\rangle$ ,  $|a\rangle$ , and  $|g\rangle$  are  $F_g = 2$ ,  $F_a = 1$ , and  $F_g = 2$ , respectively. The  $\pi$ -polarized transitions  $|g_K\rangle_\Xi \rightarrow |e_K\rangle_\Xi$  ( $K = \pm 1, \pm 2$ ) are resonant with cavity field  $\omega_e$ , the  $\pi$ -polarized transitions  $|g_K\rangle_\Xi \rightarrow |a_K\rangle_\Xi$  ( $K = 0, \pm 1$ ) are resonant with cavity field  $\omega_a$ , the  $\sigma^+$ -polarized transitions  $|g_{K-1}\rangle_\Xi \rightarrow |e_K\rangle_\Xi$  ( $K = 0, \pm 1, 2$ ) are resonant with the classical beams  $\sigma_e^+$ , and the  $\sigma^+$ -polarized transitions  $|g_{K-1}\rangle_\Xi \rightarrow |a_K\rangle_\Xi$  ( $K = 0, \pm 1$ ) are resonant with the classical beam  $\sigma_a^+$ . (b) Structure of atom  $\Lambda$ . The  $\pi$ -polarized transition  $|d\rangle_\Lambda \rightarrow |b\rangle_\Lambda$  is resonant with cavity field  $\omega_e$  and the  $\sigma^+$ -polarized transition  $|c\rangle_\Xi \rightarrow |b\rangle_\Xi$  is resonant with the classical beams  $\sigma_{bc}^+$ .

to the moving directions of the atoms. The details are shown in Figs. 4, 5, and 7. The basic principle of our protocol is encoded in the detailed steps as described in Sec. III C. In steps  $S_1^{1-3}$ , we use an atom  $\Xi$  to pass through cavities I and II sequentially. As a result, cavity II will have one photon when cavity I is initially in the excited state  $\sum_1^2 \alpha_n e^{-n\gamma t} |n\rangle$ , where we set  $n_{\max} = 2$ . Otherwise, cavity II remains in the vacuum state. In step  $S_1^4$ , we use an ancilla qubit to interact with cavity II to get an adjustable phase shift [25,31]. In step  $S_1^5$ , we use an atom  $\Xi$  to pass through cavities II and I to obtain a quantum PHASE gate, i.e., there is a phase shift only when cavity I is initially in the excited state  $\sum_1^2 \alpha_n e^{-n\gamma t} |n\rangle$  and the ancilla qubit is in the upper level. In step  $S_2^1$ , we use atom  $\Lambda$  to pass through cavities I and III. Subsequently, we use atom  $\Xi$  to pass through cavities I and II in step  $S_2^2$ . The two steps can guarantee that only when cavity I is in excited

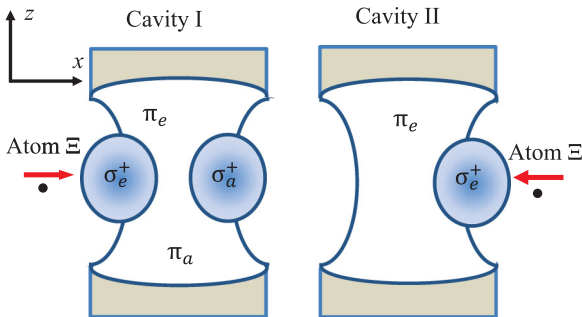


FIG. 5. Atom  $\Xi$  passes through cavities I and II. Cavity I has two resonant frequencies  $\omega_e$  and  $\omega_a$ , while cavity II has resonant frequency  $\omega_e$ . There are classical laser beams propagating through the cavities.

state  $\alpha_2 e^{-2\gamma t} |2\rangle$  initially cavity II have one photon and consequently a phase shift occurs after cavity II interacts with an ancilla qubit. Eventually, we use atom  $\Xi$  to pass through cavities II and I and then atom  $\Lambda$  to pass through cavities III and I to obtain another PHASE gate, where there can be a phase shift only when cavity I is initially in excited state  $\alpha_2 e^{-2\gamma t} |2\rangle$  and the ancilla qubit is in the upper level.

## B. Dark state and adiabatic passage

We explain the dark state and the adiabatic passage processes as follows. We consider the special case that  $n_{\max} = 2$  and the procedures here can be applied to a higher value of  $n_{\max}$ . The field state in cavity I can be expressed as

$$|\varphi\rangle = \sum_{n=0}^2 \alpha_n e^{-n\gamma t} |n\rangle_{Ie}. \quad (16)$$

As discussed before, this state results when an initial state  $\sum_{n=0}^2 \alpha_n |n\rangle_{Ie}$  undergoes a null measurement. The subscript  $Ie$  means that a photon with frequency  $\omega_e$  is in cavity I. Atom  $\Xi$  [32–39] as shown in Fig. 4(a) is a degenerate three-level atom. In a real experiment, this kind of atom has many possible candidates, such as the transition  $5^2s_{1/2}(F=3) \rightarrow 5^2p_{1/2}(F=2)$  and  $5^2p_{1/2}(F=3)$  of the  $^{85}\text{Rb}$   $D1$  line. For atom  $\Lambda$ , we can also use  $^{85}\text{Rb}$  and choose the levels  $5^2s_{1/2}(F=2, m=2)$ ,  $5^2s_{1/2}(F=3, m=3)$ , and  $5^2p_{1/2}(F=3, m=3)$ . As described in Refs. [22,34,35], atom  $\Xi$  interacts with both the cavity field  $\omega_e$  and the classical field  $\sigma_e^+$ ; hence a dark state can be written as

$$|\Psi_2^{\text{dark}}\rangle \propto |g_2\rangle_{\Xi}|2\rangle_{Ie}\Omega_2(t)\Omega_1(t) + |g_1\rangle_{\Xi}|1\rangle_{Ie}G_2^2(t)\Omega_1(t) + |g_0\rangle_{\Xi}|0\rangle_{Ie}G_2^2(t)G_1^2(t), \quad (17)$$

where

$$\Omega_K(t) = \Omega_{\Xi}(t)\langle F_g(m_g = K-1); 11|F_e(m_e = K)\rangle \quad (18)$$

are the Rabi frequencies due to the classical field  $\sigma_e^+$  and

$$G_K^n(t) = g_{\Xi}^e(t)\sqrt{n+K-2}\langle F_g(m_g = K); 10|F_e(m_e = K)\rangle \quad (19)$$

are the Rabi frequencies due to the quantum field  $\pi_e$ . The  $\langle F_g m_g; 1\sigma|F_e m_e\rangle$  are the Clebsch-Gordan coefficients for the corresponding transition channels. We can see that the dark states are dependent on the Rabi frequencies, i.e., the intensities of the classical and quantum fields. Similarly, this atom, the classical field  $\sigma_a^+$ , and the cavity field  $\omega_a$  also have a dark state just replacing  $e$  in Eq. (17) with  $a$ . The key state mapping of our proposal is the adiabatic passage within the dark states.

## C. Detailed process

In the following steps  $S_1^i$  ( $i = 1, 2, \dots, 5$ ) we present how to realize the quantum PHASE gate used in the process  $S_1$  shown in Fig. 1(a). In steps  $S_2^i$  ( $i = 1, 2$ ), we present how to realize the quantum PHASE gate used in the process  $S_2$ . Because we have assumed the maximum photon number  $n_{\max}$  to be 2, these two PHASE gates are enough to reverse the cavity state. We also discuss how to extend  $n_{\max}$  to an arbitrary number at the end of this section.



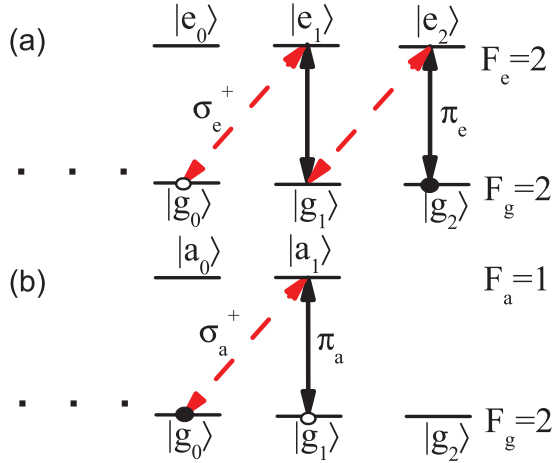


FIG. 6. Electrons moving in atom  $\Xi$  according to the adiabatic passages. Here  $\sigma_e^+$  and  $\sigma_a^+$  are classical fields, while  $\pi_e$  and  $\pi_a$  are quantum fields.

### 1. Step $S_1^1$

As shown in Fig. 5 [22], there are two classical Gaussian beams  $\sigma_e^+$  and  $\sigma_a^+$  placed at the two sides of cavity I, while in the middle, there are two quantum fields  $\pi_e$  and  $\pi_a$ . The fields' intensities are space dependent. We prepare atom  $\Xi$  initially in state  $|g_2\rangle_\Xi$  and then allow it to fly through cavity I along the  $x$  direction with a certain velocity. As the atom moves inside the cavity, under the adiabatic passage, the state of atom  $\Xi$  and cavity I evolves according to [see Fig. 6(a)]

$$\left( \sum_{n=0}^2 \alpha_n e^{-n\gamma t} |n\rangle_{Ie} \right) |g_2\rangle_\Xi \rightarrow \sum_{n=0}^2 \alpha_n e^{-n\gamma t} |0\rangle_{Ie} |g_{2-n}\rangle_\Xi. \quad (20)$$

### 2. Step $S_1^2$

As atom  $\Xi$  approaches the other side of the cavity, it encounters the classical field  $\sigma_a^+$ . Cavity I and atom  $\Xi$  will adiabatically change to [see Fig. 6(b)]

$$\left[ \alpha_0 |0\rangle_{Ia} |g_2\rangle_\Xi + \left( \sum_{n=1}^2 \alpha_n e^{-n\gamma t} |n-a\rangle_{Ia} \right) |g_1\rangle_\Xi \right] |0\rangle_{Ie}, \quad (21)$$

which means that if the initial photon number of cavity I is bigger than 0, atom  $\Xi$  will fall to state  $|g_1\rangle_\Xi$  after leaving cavity I. However, if the initial photon number is 0, atom  $\Xi$  will remain in state  $|g_2\rangle_\Xi$ .

### 3. Step $S_1^3$

Subsequently, atom  $\Xi$  enters cavity II with a classical Gaussian beam  $\sigma_e^+$  at the right side and quantum field  $\pi_e$  in the middle. As the atom moves towards the classical field, the state described by Eq. (21) evolves into

$$\left[ \alpha_0 |0\rangle_{Ia} |0\rangle_{IIe} + \left( \sum_{n=1}^2 \alpha_n e^{-n\gamma t} |n-1\rangle_{Ia} \right) |1\rangle_{IIe} \right] |0\rangle_{Ie} |g_2\rangle_\Xi. \quad (22)$$

This means that cavity II has one photon if cavity I has at least one photon initially. Otherwise, cavity II has no photon if cavity I does not have any.

### 4. Step $S_1^4$

We use an ancilla qubit [25,31] to interact with cavity II. The ancilla qubit has a down state  $|D\rangle_q$ , a upper state  $|U\rangle_q$ , and an additional state  $|A\rangle_q$ . The transition  $|U\rangle_q \rightarrow |A\rangle_q$  can interact with cavity II with a detuning  $\Delta$  (where  $\Delta \gg g_{II}$ , with  $g_{II}$  the Rabi frequency). The initial state of the ancilla qubit is prepared by the Ramsey field  $L_1$  in Fig. 3 as

$$\cos \theta |D\rangle_q + \sin \theta |U\rangle_q. \quad (23)$$

The interaction Hamiltonian has the effective form [28]

$$\hat{H}_{\text{eff}} = -\frac{\hbar g_{II}^2}{\Delta} (a_{II} a_{II}^\dagger |A\rangle\langle A| - a_{II}^\dagger a_{II} |U\rangle\langle U|), \quad (24)$$

where  $a_{II}^\dagger, a_{II}$  are the creation and annihilation operators of cavity II. After time  $\tau$ , the initial state

$$|\Psi\rangle = \left[ \alpha_0 |0\rangle_{Ia} |0\rangle_{IIe} + \left( \sum_{n=1}^2 \alpha_n e^{-n\gamma t} |n-1\rangle_{Ia} \right) |1\rangle_{IIe} \right] \otimes (\cos \theta |D\rangle_q + \sin \theta |U\rangle_q) \quad (25)$$

evolves into

$$\begin{aligned} |\Psi(t)\rangle = & \alpha_0 \cos \theta |0\rangle_{Ia} |0\rangle_{IIe} |D\rangle_q \\ & + \left( \sum_{n=1}^2 \alpha_n e^{-n\gamma t} |n-1\rangle_{Ia} \right) \cos \theta |1\rangle_{IIe} |D\rangle_q \\ & + \alpha_0 \sin \theta |0\rangle_{Ia} |0\rangle_{IIe} |U\rangle_q \\ & + e^{(-ig_{II}^2/\Delta)\tau} \left( \sum_{n=1}^2 \alpha_n e^{-n\gamma t} |n-1\rangle_{Ia} \right) \sin \theta |1\rangle_{IIe} |U\rangle_q. \end{aligned} \quad (26)$$

A phase element  $e^{(-ig_{II}^2/\Delta)\tau}$  appears when  $n \geq 1$  and the ancilla qubit is in the excited state.

### 5. Step $S_1^5$

At this stage, we prepare an atom  $\Xi$  in  $|g_2\rangle_\Xi$  and move it in the opposite direction of  $x$  to pass through cavities II and I [22,34,35]. The atom and cavity will undergo symmetric transmissions from step  $S_1^3$  to step  $S_1^1$ . After atom  $\Xi$  passes through cavity II, cavity II will be back to the vacuum state and the whole state will be

$$\begin{aligned} |\Psi(t)\rangle = & \alpha_0 \cos \theta |0\rangle_{Ia} |g_2\rangle_\Xi |D\rangle_q \\ & + \left( \sum_{n=1}^2 \alpha_n e^{-n\gamma t} |n-1\rangle_{Ia} \right) \cos \theta |g_1\rangle_\Xi |D\rangle_q \\ & + \alpha_0 \sin \theta |0\rangle_{Ia} |g_2\rangle_\Xi |U\rangle_q \\ & + e^{(-ig_{II}^2/\Delta)\tau} \left( \sum_{n=1}^2 \alpha_n e^{-n\gamma t} |n-1\rangle_{Ia} \right) \sin \theta |g_1\rangle_\Xi |U\rangle_q. \end{aligned} \quad (27)$$

After passing through cavity I, atom  $\Xi$  will be back to  $|g_2\rangle_\Xi$ . The final state reads

$$\begin{aligned}
 |\Psi(t)\rangle = & \alpha_0 \cos \theta |0\rangle_{1e} |D\rangle_q \\
 & + \left( \sum_{n=1}^2 \alpha_n e^{-n\gamma t} |n\rangle_{1e} \right) \cos \theta |D\rangle_q + \alpha_0 \sin \theta |0\rangle_{1e} |U\rangle_q \\
 & + e^{(-ig_{II}^2/\Delta)\tau} \left( \sum_{n=1}^2 \alpha_n e^{-n\gamma t} |n\rangle_{1e} \right) \sin \theta |U\rangle_q. \quad (28)
 \end{aligned}$$

The above processes show that we can obtain a quantum PHASE gate.

### 6. Step $S_2^1$

We can improve the above proposal and guarantee that only when the photon number is bigger than 1 can there be a phase shift. Achieving this goal, we need another kind of atom  $\Lambda$  as shown in Fig. 4(b). Having  $M$  number of atoms  $\Lambda$ , they and cavity I also have a dark state reading ( $n \geq M$ ) [22,28]

$$\begin{aligned}
 |\Psi_n^{\text{dark}}\rangle \propto & [-\Omega_\Lambda(t)/g_\Lambda(t)]^M |d \cdots d\rangle_{1e} \sqrt{(n-M)!}/\sqrt{n!} \\
 & + [-\Omega_\Lambda(t)/g_\Lambda(t)]^{M-1} \sum_{i=1}^M |d \cdots c_i \cdots d\rangle_{1e} \\
 & \times \sqrt{(n-M)!}/\sqrt{(n-1)!} + \cdots + |c \cdots c\rangle_{1e} |n-M\rangle_{1e}, \quad (29)
 \end{aligned}$$

where  $\Omega_\Lambda$  is the Rabi frequency between the classical field and dipole  $|b\rangle_\Lambda \leftrightarrow |c\rangle_\Lambda$  and  $g_\Lambda$  is the Rabi frequency between the quantum field with one photon and dipole  $|b\rangle_\Lambda \leftrightarrow |d\rangle_\Lambda$ .

$$\begin{aligned}
 \left( \sum_{n=0}^2 \alpha_n e^{-n\gamma t} |n\rangle_{1e} \right) |d\rangle_\Lambda |g_2\rangle_\Xi & \xrightarrow{\text{cavity I}} [(\alpha_0 |d\rangle_\Lambda + \alpha_1 e^{-\gamma t} |c\rangle_\Lambda) |0\rangle_{1e} + \alpha_2 e^{-2\gamma t} |c\rangle_\Lambda |1\rangle_{1e}] |g_2\rangle_\Xi \\
 & \xrightarrow{\text{cavity III}} [(\alpha_0 |0\rangle_{IIIe} + \alpha_1 e^{-\gamma t} |1\rangle_{IIIe}) |0\rangle_{1e} + \alpha_2 e^{-2\gamma t} |1\rangle_{IIIe} |1\rangle_{1e}] |d\rangle_\Lambda |g_2\rangle_\Xi \\
 & \xrightarrow{\text{cavity II}} [(\alpha_0 |0\rangle_{IIIe} + \alpha_1 e^{-\gamma t} |1\rangle_{IIIe}) |0\rangle_{IIe} + \alpha_2 e^{-2\gamma t} |1\rangle_{IIIe} |1\rangle_{IIe}] |0\rangle_{1e} |d\rangle_\Lambda |g_2\rangle_\Xi, \quad (31)
 \end{aligned}$$

where cavity I and cavity III on the arrows denote the state after atom  $\Lambda$  passes through cavity II and III. Meanwhile cavity II denotes the state after atom  $\Xi$  passes through cavity II. It shows that only when the initial photon number is bigger than 1 can cavity II have one photon and consequently there can be a phase shift as we discussed in step  $S_1^4$ .

Next we map the coherence stored in cavities II and III back to cavity I. First, we prepare atom  $\Xi$  in state  $|g_2\rangle_\Xi$  to fly through cavities II and I as in step  $S_1^5$ . Second, we prepare atom  $\Lambda$  in state  $|d\rangle_\Lambda$  to pass through cavities III and I. The atom will carry the photon back to cavity I if cavity III has a photon.

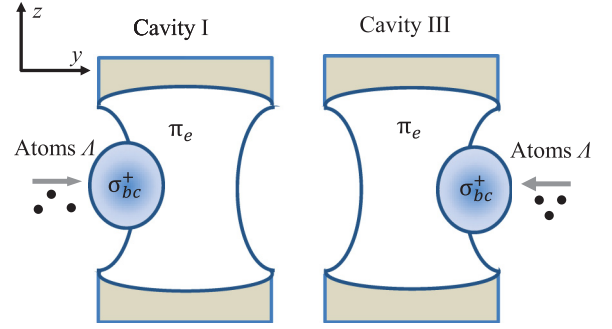


FIG. 7. Atoms  $\Lambda$  pass through cavities I and III. Cavity III has resonant frequency  $\omega_e$ . There are classical laser beams propagating through the cavities.

As shown in Fig. 7, at the beginning, we let one atom  $\Lambda$  prepared in state  $|d\rangle_\Lambda$  to move along the  $y$  direction and pass through cavity I. The atom encounters the classical field  $\sigma_{bc}^+$  and then the quantum field  $\pi_e$ . The state evolves according to

$$|d\rangle_\Lambda |n\rangle_{1e} \rightarrow |c\rangle_\Lambda |n-1\rangle_{1e}. \quad (30)$$

Then atom  $\Lambda$  enters cavity III interacting with quantum field  $\pi_e$  in the middle and classical field  $\sigma_{bc}^+$  at the right side. As a result, atom  $\Lambda$  emits one photon into cavity III. This means that we store one photon in cavity III if the initial photon number of cavity I is larger than 0.

### 7. Step $S_2^2$

Based on the outcome in step  $S_2^1$ , there will be one photon in cavity I if it has two photons initially. Otherwise, cavity I will have no photon. Now atom  $\Xi$  flies through cavities I and II. It will experience steps  $S_1^{1-3}$  as before. The whole state evolves as

Our protocol also can be extended to a larger  $n_{\max}$  and only when the photon number is bigger than  $s$  can there be a PHASE gate. We just need to add  $s$  atoms  $\Lambda$  to pass through cavities I and III to store at most  $s$  photons in cavity III. Subsequently, we do steps  $S_1^{1-5}$  and we can obtain a PHASE gate. Of course, in this process, we should choose atom  $\Xi$  to have suitable total angular momentum.

## IV. PROTOCOL TO REVERSE WEAK MEASUREMENT WITH ARBITRARY MAXIMUM PHOTON NUMBER

In this section we show how to reverse weak measurement with arbitrary maximum photon number by using the quantum PHASE gates realized in the previous section. In Eq. (28) we

show that we can get the quantum PHASE gate

$$Q_\pi = \begin{pmatrix} 1 & 0 & 0 & 0 \\ 0 & 1 & 0 & 0 \\ 0 & 0 & 1 & 0 \\ 0 & 0 & 0 & -1 \end{pmatrix} \quad (32)$$

by setting  $\tau = \frac{\pi\Delta}{g_{II}^2}$ . Similar to Ref. [25], before the ancilla qubit interacts with cavity II, we do a Hadamard gate (by Ramsey field  $L_2$  in Fig. 3)

$$H_\beta = \begin{pmatrix} \cos \beta & -\sin \beta & 0 & 0 \\ \sin \beta & \cos \beta & 0 & 0 \\ 0 & 0 & \cos \beta & -\sin \beta \\ 0 & 0 & \sin \beta & \cos \beta \end{pmatrix} \quad (33)$$

on the ancilla qubit. After the interaction, we do another Hadamard gate (by Ramsey field  $L_3$  in Fig. 3) on the ancilla qubit. We can construct a CNOT gate of Eq. (4) by  $H_{\pi/4} Q_\pi H_{-\pi/4}$  [see Fig. 1(b)]. The total effects of these quantum gates yield the state shown in Eq. (26),

$$\begin{aligned} |\Psi(t)\rangle = & \alpha_0 \cos \theta |0\rangle_{Ia} |0\rangle_{IIe} |D\rangle_q \\ & + \left( \sum_{n=1}^2 \alpha_n e^{-n\gamma t} |n-1\rangle_{Ia} \right) \sin \theta |1\rangle_{IIe} |D\rangle_q \\ & + \alpha_0 \sin \theta |0\rangle_{Ia} |0\rangle_{IIe} |U\rangle_q \\ & + \left( \sum_{n=1}^2 \alpha_n e^{-n\gamma t} |n-1\rangle_{Ia} \right) \cos \theta |1\rangle_{IIe} |U\rangle_q. \end{aligned} \quad (34)$$

Next we measure the ancilla qubit and determine the reversal of the quantum field state as in Eqs. (6)–(9). Then we do step  $S_1^5$  in the previous section to obtain the cavity state shown in Eq. (6). Subsequently, we do steps  $S_2^{1,2}$  in the previous section followed by Eq. (34). Finally, we can reverse the quantum field state.

As we discussed at the end of the previous section, we can extend our proposal to a large value of  $n_{\max}$  by simply repeating the above procedures.

Our proposal requires the lifetime of the cavities and atoms to be much longer than the total time of the reversal process, which is limited by the cavity quality factor and

atom-cavity coupling strength. In our proposal, the atoms are always in the ground state, so the atoms are sometimes long lived. Recently, strong coupling between a single atom and monolithic microresonator was observed [40]. Ultrahigh-quality cavities also have been demonstrated with a quality factor up to  $10^9$  in a wedge resonator on a silicon chip with a dimensional size of hundreds of micrometers [41] and  $10^{11}$  in a calcium fluoride whispering gallery mode optical resonator with a size of several millimeters [42]. This means that the cavity lifetime can reach  $100 \mu s$ . If the atom velocity reaches thousands of meters per second, the time it takes for the atom to pass through the cavity is about  $1 \mu s$ . If  $n_{\max} = 2$ , the total reversal time will be about  $20 \mu s$ , including the projecting measurement time on the ancilla qubit set to  $1 \mu s$ . This means that the cavity lifetime can be much longer than the time of the reversal procedure. With the progress of nanofabrication technology [41], our proposal may be realized with improved experimental parameters in the near future.

## V. CONCLUSION

In summary, we have proposed a protocol to reverse the weak measurement of a cavity field with arbitrary maximum photon number, which may have important applications in high-dimensional quantum information based on a real system. Taking advantage of the adiabatic passage within the dark states, we can realize quantum PHASE gates and subsequently CNOT gates between the cavity field and an ancilla qubit, which play a key role in the reversion. The success probability of our proposal to reverse the state approaches  $e^{-2n_{\max}\gamma t}$ .

Finally, we note that, compared to the proposal in Ref. [22], this proposal involves more devices and is technically harder. However, the advantage of this protocol is that our method does not need any other weak measurement and consequently can accelerate the reversal process, which is very important in many applications.

## ACKNOWLEDGMENTS

This research was supported by NPRP Grant No. 7-210-1-032 from the Qatar National Research Fund and a grant from King Abdulaziz City for Science and Technology.

- 
- [1] M. Ueda and M. Kitagawa, *Phys. Rev. Lett.* **68**, 3424 (1992).
  - [2] A. Imamoglu, *Phys. Rev. A* **47**, R4577(R) (1993).
  - [3] A. N. Korotkov, *Phys. Rev. B* **60**, 5737 (1999).
  - [4] A. N. Jordan and A. N. Korotkov, *Contemp. Phys.* **51**, 125 (2010).
  - [5] Y. P. Zhong, Z. L. Wang, J. M. Martinis, A. N. Cleland, A. N. Korotkov, and H. Wang, *Nat. Commun.* **5**, 3135 (2014).
  - [6] K. Keane and A. N. Korotkov, *Phys. Rev. A* **86**, 012333 (2012).
  - [7] A. N. Korotkov and K. Keane, *Phys. Rev. A* **81**, 040103(R) (2010).
  - [8] E. Knill, *Nature (London)* **434**, 39 (2005).
  - [9] J. C. Lee, Y. C. Jeong, Y. S. Kim, and Y. H. Kim, *Opt. Express* **19**, 16309 (2011).
  - [10] Y. S. Kim, J. C. Lee, O. Kwon, and Y. H. Kim, *Nat. Phys.* **8**, 117 (2011).
  - [11] Q. Sun, M. Al-Amri, L. Davidovich, and M. S. Zubairy, *Phys. Rev. A* **82**, 052323 (2010).
  - [12] X. L. Zong, C. Q. Du, M. Yang, Q. Yang, and Z. L. Cao, *Phys. Rev. A* **90**, 062345 (2014).
  - [13] S. C. Wang, Z. W. Yu, W. J. Zou, and X. B. Wang, *Phys. Rev. A* **89**, 022318 (2014).
  - [14] C. M. Yao, Z. H. Ma, Z. H. Chen, and A. Serafini, *Phys. Rev. A* **86**, 022312 (2012).
  - [15] Z. X. Man, Y. J. Xia, and N. B. An, *Phys. Rev. A* **86**, 012325 (2012).
  - [16] D. J. Starling and N. S. Williams, *Phys. Rev. A* **88**, 024304 (2013).

- [17] Z. He, C. M. Yao, and J. Zou, *Phys. Rev. A* **88**, 044304 (2013).
- [18] Y. S. Kim, Y. W. Cho, Y. S. Ra, and Y. H. Kim, *Opt. Express* **17**, 11978 (2009).
- [19] A. Royer, *Phys. Rev. Lett.* **73**, 913 (1994).
- [20] M. A. Nielsen and C. M. Caves, *Phys. Rev. A* **55**, 2547 (1997).
- [21] A. N. Korotkov and A. N. Jordan, *Phys. Rev. Lett.* **97**, 166805 (2006).
- [22] Q. Sun, M. Al-Amri, and M. S. Zubairy, *Phys. Rev. A* **80**, 033838 (2009).
- [23] N. Katz, M. Neeley, M. Ansmann, R. C. Bialczak, M. Hofheinz, E. Lucero, A. O'Connell, H. Wang, A. N. Cleland, J. M. Martinis, and A. N. Korotkov, *Phys. Rev. Lett.* **101**, 200401 (2008).
- [24] M. Koashi and M. Ueda, *Phys. Rev. Lett.* **82**, 2598 (1999).
- [25] M. Al-Amri, M. O. Scully, and M. S. Zubairy, *J. Phys. B* **44**, 165509 (2011).
- [26] J. von Neumann, *Mathematical Foundations of Quantum Mechanics* (Princeton University Press, Princeton, 1955).
- [27] A. Barchielli and V. P. Belavkin, *J. Phys. A: Math. Gen.* **24**, 1495 (1991).
- [28] M. O. Scully and M. S. Zubairy, *Quantum Optics* (Cambridge University Press, New York, 1997).
- [29] F. L. Li, H. Xiong, and M. S. Zubairy, *Phys. Rev. A* **72**, 010303(R) (2005).
- [30] H. Xiong, M. O. Scully, and M. S. Zubairy, *Phys. Rev. Lett.* **94**, 023601 (2005).
- [31] A. Rauschenbeutel, G. Nogues, S. Osnaghi, P. Bertet, M. Brune, J. M. Raimond, and S. Haroche, *Phys. Rev. Lett.* **83**, 5166 (1999).
- [32] A. Sargsyan, G. Hakhumyan, C. Leroy, Y. Pashayan-Leroy, A. Papoyan, D. Sarkisyan, and M. Auzinsh, *J. Opt. Soc. Am. B* **31**, 1046 (2014).
- [33] D. A. Steck, Rubidium 85 D line data, 2009, <http://steck.us/alkalidata>.
- [34] A. S. Parkins, P. Marte, P. Zoller, and H. J. Kimble, *Phys. Rev. Lett.* **71**, 3095 (1993).
- [35] A. S. Parkins, P. Marte, P. Zoller, O. Carnal, and H. J. Kimble, *Phys. Rev. A* **51**, 1578 (1995).
- [36] J. Martin, B. W. Shore, and K. Bergmann, *Phys. Rev. A* **54**, 1556 (1996).
- [37] W. Lange and H. J. Kimble, *Phys. Rev. A* **61**, 063817 (2000).
- [38] B. Wang, Y. Han, J. Xiao, X. Yang, C. Zhang, H. Wang, M. Xiao, and K. Peng, *Phys. Rev. A* **75**, 051801(R) (2007).
- [39] E. Vaz and J. Kyriakidis, *Phys. Rev. B* **86**, 235310 (2012).
- [40] T. Aoki, B. Dayan, E. Wilcut, W. P. Bowen, A. S. Parkins, T. J. Kippenberg, K. J. Vahala, and H. J. Kimble, *Nature (London)* **443**, 671 (2006).
- [41] H. Lee, T. Chen, J. Li, K. Y. Yang, S. Jeon, O. Painter, and K. J. Vahala, *Nat. Photon.* **6**, 369 (2012).
- [42] A. A. Savchenkov, A. B. Matsko, V. S. Ilchenko, and L. Maleki, *Opt. Express* **15**, 006768 (2007).